Semnan University

Journal of Heat and Mass Transfer Research

Journal homepage: http://jhmtr.journals.semnan.ac.ir

Analytical and Numerical Studies on Hydromagnetic Flow of Boungiorno Model Nanofluid over a Vertical Plate

B. Ganga, S. Mohamed Yusuff Ansari, N.Vishnu Ganesh, A.K. Abdul Hakeem*

Department of Mathematics,Providence College for Women, Coonoor - 643 104, INDIA.
Department of Mathematics, Jamal Mohamed College, Trichy - 620 020, INDIA.
Department of Mathematics, Sri Ramakrishna Mission Vidyalaya College of Arts & Science, Coimbatore - 641 020, INDIA.

PAPER INFO

History:

Submitted 25 September 2015
Received 6 January 2015
Accepted 6 August 2016

Keywords:

Homotopy analysis method
Magnetohydrodynamics
Nanofluid
Runge–Kutta method
Vertical plate

A B S T R A C T

The magnetohydrodynamic boundary-layer flow of two-phase model nanofluid over a vertical plate is investigated both analytically and numerically. A system of governing nonlinear partial differential equations is converted into a set of nonlinear ordinary differential equations by suitable similarity transformations, and the transformed equations are solved analytically using the homotopy analysis method and numerically by the fourth-order Runge–Kutta method along with a shooting technique. The effects of pertinent physical parameters on velocity, temperature, and concentration profiles of the nanofluid are discussed graphically. Furthermore, comparisons have been made with benchmark solutions for a special case and have obtained very good agreement.

DOI: 10.22075/jhmtr.2016.362

1. Introduction

The flow of nanofluid is of great interest in many areas of modern science: engineering and technology, chemical and nuclear industries, and biomechanics. Nanofluids are not obtained naturally, but they are synthesized in a laboratory. Modern nanotechnology provides opportunities to process and produce ultra-fine solid particles with a diameter less than 50 nm. Fluids with ultra-fine solid particles (nanoparticles) suspended in them are called nanofluids, which is a term coined in 1995 by Choi of the Argonne National Laboratory, U.S.A. [1]. Nanofluids can be considered as the next-generation heat-transfer fluids, as they offer exciting new possibilities to enhance heat-transfer performance compared to pure liquids. This concept attracted various researchers to nanofluids, and various theoretical and experimental studies have been performed to find the thermal properties of nanofluids [2-15].

Kuznetsov and Nield [16] studied the classical problem of free convection boundary-layer flow of viscous and incompressible fluids passed through a vertical flat plate in the case of two-phase model nanofluids. The same authors [17] extended their investigation to study the double-diffusive natural convection boundary-layer flow of nanofluid over a vertical plate. Khan and Pop [18] analyzed the development of steady boundary-layer flow, heat transfer, and nanoparticle volume fraction over a linear stretching surface in a nanofluid. Khan and

Corresponding Author: *A.K. Abdul Hakeem Department of Mathematics, Sri Ramakrishna Mission Vidyalaya College of Arts & Science, Coimbatore - 641 020, INDIA*
Email: abdulhakeem6@gmail.com

Aziz [19] investigated the boundary-layer flow of nanofluid past a vertical surface with a constant heat flux. Gorla and Chamkha [20] analyzed the natural convection flow of a nanofluid past an isothermal horizontal plate in a porous medium saturated by a nanofluid. Aziz and Khan [21] studied the natural convection flow of a nanofluid over a convectively heated vertical plate.

The applied magnetic field may play an important role in controlling momentum and heat transfers in the boundary-layer flow of different fluids. Ibrahim et al. [22] investigated the magnetic-field effects on free convection and mass-transfer flow past a semi-infinite vertical flat plate. Muthucumaraswamy and Janakiraman [23] studied the thermal-radiation effects on flow past an impulsively started infinite vertical plate with uniform temperature and variable mass diffusion in the presence of a transverse-applied magnetic field. Yahyazadeh et al. [24] inspected the effect of a magnetic field on the free convection flow of a nanofluid over a linear stretching sheet.

Nonlinear phenomena play a crucial role in applied mathematics and physics. The theory of nonlinear problems recently has been the focus of many studies. In most cases, it is difficult to solve nonlinear problems, especially to obtain the analytical solutions. An analytical method for strongly nonlinear problems, namely the homotopy analysis method (HAM), was proposed by Liao in 1992. The HAM is a general analytic approach to derive a series of solutions for various types of nonlinear equations, including algebraic equations, ordinary differential equations, partial differential equations, differential-integral equations, differential-difference equations, and coupled equations. Unlike perturbation methods, the HAM is independent of small or large physical parameters and, thus, is valid whether or not a nonlinear problem contains small or large physical parameters. More importantly, different from all perturbation and traditional non perturbation methods, the HAM provides a simple way to ensure the convergence of a solution series, and therefore, the HAM is valid even for strongly nonlinear problems. In addition, the HAM provides great freedom to choose proper base functions to approximate a nonlinear problem [25-32]. Motivated by the advantages of the HAM, we have applied it to investigate the boundary-layer flow of an incompressible, viscous nanofluid over a vertical plate in the presence of the magnetic-field effect. To verify the HAM solutions, we have compared the present solutions with the numerical solutions obtained by the fourth-order Runge–Kutta method along with the shooting iteration technique.

2. Formulation of the problem

Consider the steady two-dimensional boundary-layer flow of a nanofluid over a vertical plate in the presence of a magnetic field. We select a coordinate frame in which the x axis is aligned vertically upwards. We consider a vertical plate at $y = 0$. At this boundary, the temperature T and the nanoparticle volume fraction ϕ take constant values T_w and ϕ_w, respectively. The temperature T and the nanoparticle volume fraction of the nanofluid ϕ take values T_∞ and ϕ_∞,respectively, as $y\to\infty$. We also consider the influence of a constant magnetic-field strength B_0, which is applied normally to the plate. It is assumed further that the induced magnetic field is negligible in comparison to the applied magnetic field. Under the above assumptions, the boundary-layer equations governing the flow and thermal and concentration fields can be written in dimensional form as follows [16]:

$$\frac{\partial u}{\partial x}+\frac{\partial v}{\partial y}=0, \tag{1}$$

$$\begin{aligned}&\frac{\partial p}{\partial x}=\mu\frac{\partial^2 u}{\partial y^2}\\&-\rho_f\left(u\frac{\partial u}{\partial x}+v\frac{\partial u}{\partial y}\right)-\sigma B_0^2 u\\&+\left[(1-\phi_\infty)\rho_{f\infty}\beta g(T-T_\infty)-(\rho_p-\rho_{f\infty})g(\phi-\phi_\infty)\right],\end{aligned} \tag{2}$$

$$u\frac{\partial T}{\partial x}+v\frac{\partial T}{\partial y}=\alpha\nabla^2 T+\tau\left[D_B\frac{\partial\phi}{\partial y}\frac{\partial T}{\partial y}+\frac{D_T}{T_\infty}\left(\frac{\partial T}{\partial y}\right)^2\right], \tag{3}$$

$$u\frac{\partial\phi}{\partial x}+v\frac{\partial\phi}{\partial y}=D_B\left(\frac{\partial^2\phi}{\partial y^2}\right)+\frac{D_T}{T_\infty}\left(\frac{\partial^2 T}{\partial y^2}\right), \tag{4}$$

where u and v are the velocity components along the x and y directions, respectively, p is the fluid pressure, ρ_f is the density of the base fluid, ρ_p is the nanoparticle density, μ is the absolute viscosity of the base fluid, $\alpha=\frac{k}{(\rho c)_f}$ is the thermal diffusivity of the base fluid, $\tau=\frac{(\rho c)_p}{(\rho c)_f}$ is the ratio of nanoparticle heat capacity and the base fluid heat capacity, ϕ is

the local solid volume fraction of the nanofluid, β is the volumetric thermal expansion coefficient of the base fluid, D_B is the Brownian diffusion coefficient, $D_T$is the thermophoretic diffusion coefficient, T is the local temperature, g is the acceleration due to gravity, and B_0 is the constant magnetic field.

The boundary conditions are taken to be

$$u = 0,\ v = 0,\ T = T_w,\ \phi = \phi_w \text{ at } y = 0, \quad (5)$$

$$u = v = 0,\ T = T_\infty,\ \phi = \phi_\infty \text{ as } y \to \infty. \quad (6)$$

3. **Similarity transformations**

The following quantities are introduced to transform Eqs. (2)–(4) into ordinary differential equations:

$$\eta = \frac{y}{x} Ra_x^{1/4},\ \psi = aRa_x^{1/4} s(\eta),$$

$$\theta(\eta) = \frac{T - T_\infty}{T_w - T_\infty},\ f(\eta) = \frac{\phi - \phi_\infty}{\phi_w - \phi_\infty},$$

(10)

with the local Rayleigh number, which is defined as

$$Ra_x = \frac{(1-\phi_\infty) g\beta (T_w - T_\infty) x^3}{\nu a}, \quad (11)$$

and the stream function $\psi(x,y)$ is defined such that

$$u = \frac{\partial \psi}{\partial y},\ v = -\frac{\partial \psi}{\partial x}. \quad (12)$$

Therefore, the continuity equation from Eq. (1) is satisfied identically. After some algebraic manipulation, the momentum, energy, and solid-volume fraction equations are obtained as follows:

$$s''' + \frac{1}{4\,\mathrm{Pr}}\left(3ss'' - 2s'^2 - 4M\sqrt{\mathrm{Pr}}s'\right) + \theta - Nrf = 0, \quad (13)$$

$$\theta'' + \frac{3}{4} s\theta' + Nbf'\theta' + Nt\theta'^2 = 0, \quad (14)$$

$$f'' + \frac{3}{4} Le\, s\, f' + \frac{Nt}{Nb}\theta'' = 0, \quad (15)$$

where primes denote differentiation with respect to η and the nondimensional parameters—the Prandtl number (*Pr*), buoyancy-ratio parameter (*Nr*), Brownian motion parameter (*Nb*), thermophoresis parameter (*Nt*), Lewis number (*Le*), and magnetic parameter(*M*)—are defined as follows:

$$\mathrm{Pr} = \frac{\nu}{\alpha},\ Nr = \frac{(\rho_p - \rho_{f\infty})(\phi_w - \phi_\infty)}{\rho_{f\infty}\beta(T_w - T_\infty)(1-\phi_\infty)},$$

$$Nb = \frac{(\rho c)_p D_B (\phi_w - \phi_\infty)}{(\rho c)_f \alpha},\ Nt = \frac{(\rho c)_p D_T (T_w - T_\infty)}{(\rho c)_f \alpha T_\infty},$$

$$Le = \frac{\alpha}{D_B} \text{ and } M = \frac{\sigma B_0^2 x^{1/2}}{\rho_f \sqrt{(1-\phi_\infty) g\beta (T_w - T_\infty)}}.$$

The corresponding boundary conditions are as follows:

$$s(\eta) = s'(\eta) = 0,\ \theta(\eta) = f(\eta) = 1 \text{ at } \eta = 0, \quad (16)$$

$$s'(\eta) = 0,\ \theta(\eta) = 0,\quad f(\eta) = 0 \text{ as } \eta \to \infty. \quad (17)$$

The reduced local Nusselt number *Nur* and the reduced local Sherwood number *Shr* can be introduced and represented as follows:

$$Nur = Ra_x^{1/4} Nu = -\theta'(0)$$

$$Shr = Ra_x^{1/4} Sh = -f'(0).$$

4. Analytical solution by the HAM

Eqs. (13)–(15) are solved under corresponding boundary conditions (16) and (17) by using the HAM. For the HAM solutions, we choose the initial guesses and auxiliary linear operators in the following form:

$$s_0(\eta) = 1 - e^{-\eta} - \eta e^{-\eta},\ \theta_0(\eta) = e^{-\eta},$$

$$f_0(\eta) = e^{-\eta}, \quad (20)$$

$$L_1(s) = s''' - s',\ L_2(\theta) = \theta'' + \theta,$$

$$L_3(f) = f'' + f, \quad (21)$$

and

$$L_1\left(c_1 + c_2 e^{\eta} + c_3 e^{-\eta}\right) = L_2\left(c_1 e^{\eta} + c_2 e^{-\eta}\right) = 0$$

$$L_3\left(c_1 e^{\eta} + c_2 e^{-\eta}\right) = 0. \quad (22)$$

c_1, c_2,and c_3 are constants, $p \in [0,1]$ denotes the embedding parameter, and h_1, h_2, and h_3 indicate the

nonzero auxiliary parameters. We then construct the following problems:

Zeroth-order deformation problems,

$$\begin{aligned}&(1-p)L_1[s(\eta,p)-s_0(\eta)]\\&=ph_1N_1[s(\eta,p),\theta(\eta,p),f(\eta,p)],\end{aligned}\tag{23}$$

$$\begin{aligned}&(1-p)L_2[\theta(\eta,p)-\theta_0(\eta)]\\&=ph_2N_2[s(\eta,p),\theta(\eta,p),f(\eta,p)],\end{aligned}$$

(24)

$$\begin{aligned}&(1-p)L_3[f(\eta,p)-f_0(\eta)]\\&=ph_3N_3[s(\eta,p),\theta(\eta,p),f(\eta,p)],\end{aligned}$$

(25)

$$s(0,p)=0,\ s'(0,p)=0,\ s'(\infty,p)=0,\tag{26}$$

$$\theta(0,p)=1,\ \theta(\infty,p)=0,\tag{27}$$

$$f(0,p)=1,\ f(\infty,p)=0,\tag{28}$$

and

$$\begin{aligned}&N_1[s(\eta,p),\theta(\eta,p),f(\eta,p)]\\&=s'''(\eta,p)\\&+\frac{1}{4\,\mathrm{Pr}}\left(3s(\eta,p)s''(\eta,p)-2s'^2(\eta,p)-4M\sqrt{\mathrm{Pr}}s'(\eta,p)\right)\\&+\theta(\eta,p)-Nrf(\eta,p),\end{aligned}\tag{29}$$

$$\begin{aligned}&N_2[s(\eta,p),\theta(\eta,p),f(\eta,p)]=\theta''(\eta,p)\\&+\frac{3}{4}s(\eta,p)\theta'(\eta,p)+Nbf'(\eta,p)\theta'(\eta,p)\\&+Nt\theta'^2(\eta,p),\end{aligned}\tag{30}$$

$$\begin{aligned}&N_3[s(\eta,p),\theta(\eta,p),f(\eta,p)]=f''(\eta,p)\\&+\frac{3}{4}Les(\eta,p)f'(\eta,p)+\frac{Nb}{Nt}\theta''(\eta,p).\end{aligned}\tag{31}$$

For p = 0 and p = 1, we have

$$s(\eta,0)=s_0(\eta),\ s(\eta,1)=s(\eta)$$

(32)

$$\theta(\eta,0)=\theta_0(\eta),\ \theta(\eta,1)=\theta(\eta)\tag{33}$$

$$f(\eta,0)=f_0(\eta),\ f(\eta,1)=f(\eta).\tag{34}$$

Due to the Taylor series with respect to p,the following is provided:

$$s(\eta,p)=s_0(\eta)+\sum_{m=1}^{\infty}s_m(\eta)p^m,$$

(35)

$$\theta(\eta,p)=\theta_0(\eta)+\sum_{m=1}^{\infty}\theta_m(\eta)p^m,\tag{36}$$

$$f(\eta,p)=f_0(\eta)+\sum_{m=1}^{\infty}f_m(\eta)p^m,\tag{37}$$

$$s_m(\eta)=\frac{1}{m!}\frac{\partial^m(s(\eta,p))}{\partial p^m},\tag{38}$$

$$\theta_m(\eta)=\frac{1}{m!}\frac{\partial^m(\theta(\eta,p))}{\partial p^m},\tag{39}$$

$$f_m(\eta)=\frac{1}{m!}\frac{\partial^m(f(\eta,p))}{\partial p^m},\tag{40}$$

and thus, the m[th]-order deformation problems are as follows:

$$L_1[s_m(\eta)-\chi_m s_{m-1}(\eta)]=h_1R_m^s(\eta),\tag{41}$$

$$L_2[\theta_m(\eta)-\chi_m\theta_{m-1}(\eta)]=h_2R_m^\theta(\eta),\tag{42}$$

$$L_3[f_m(\eta)-\chi_m f_{m-1}(\eta)]=h_3R_m^f(\eta),\tag{43}$$

and

$$s_m(0)=s_m'(0)=s_m'(\infty)=0\ ,\tag{44}$$

$$\theta_m(0)=\theta_m(\infty)=0\,,\tag{45}$$

$$f_m(0)=f_m(\infty)=0\,,\tag{46}$$

where

$$\begin{aligned}&R_m^s=s_{m-1}'''\\&+\frac{1}{4\,\mathrm{Pr}}\left(3\sum_{i=0}^{m-1}s_{m-1-i}s_i''-2\sum_{i=0}^{m-1}s_{m-1-i}'s_i'-4M\sqrt{\mathrm{Pr}}s_{m-1}'\right)\\&+\theta_{m-1}-Nrf_{m-1}\end{aligned}\tag{47}$$

$$\begin{aligned}&R_m^\theta=\theta_{m-1}''+\frac{3}{4}\sum_{i=0}^{m-1}s_{m-1-i}\theta_i'\\&+Nb\sum_{i=0}^{m-1}f_{m-1-i}'\theta_i'+Nt\sum_{i=0}^{m-1}\theta_{m-1-i}'\theta_i'\end{aligned}\tag{48}$$

$$R_m^f=f_{m-1}''+\frac{3}{4}Le\sum_{i=0}^{m-1}s_{m-1-i}f_i'+\frac{Nt}{Nb}\theta_{m-1}''\tag{49}$$

and

$$\chi_m = \begin{cases} 0(m \le 1) \\ 1(m > 1) \end{cases}, \tag{50}$$

for which *h* is chosen in such a way that these three series are convergent at p = 1.Therefore,we have

$$s(\eta) = s_0(\eta) + \sum_{m=1}^{\infty} s_m(\eta), \tag{51}$$

$$\theta(\eta) = \theta_0(\eta) + \sum_{m=1}^{\infty} \theta_m(\eta), \tag{52}$$

$$f(\eta) = f_0(\eta) + \sum_{m=1}^{\infty} f_m(\eta). \tag{53}$$

4.1 Convergence of the HAM

As Liao [24-26] has pointed out, the convergence rate of approximation for the HAM solution strongly depends on the value of auxiliary parameter *h*. Fig. 1 clearly depicts that the range for the admissible value of *h* is -1.1 ≤ h ≤ -0.1. Our calculation for this case indicates that *h*= -0.3 for the whole region η.

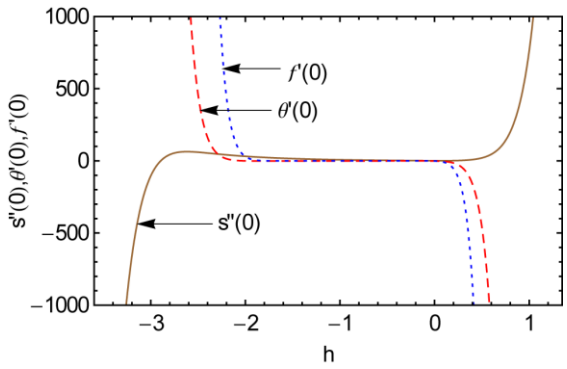

Fig.1 s′′(0), θ ′(0), and f ′(0) plots for determining the optimum *h* coefficient.

5. Numerical method for the solution

Nonlinear coupled differential Eqs.(13)–(15), along with boundary conditions (16) and (17), form a two-point boundary value problem thatis solved using a shooting technique along with the fourth-order Runge–Kutta integration scheme by converting it into an initial value problem. In this method, we have to choose a suitable finite value of $\eta \to \infty$, say η_∞.We set the following first-order system:

$$y_1' = y_2,\ y_2' = y_3,$$

$$y_3' = -\frac{1}{4\,\mathrm{Pr}}\left(3y_1y_3 - 2y_2^2 - 4M\sqrt{\mathrm{Pr}}\,y_2\right) - y_4 + Nry_6,$$

$$y_4' = y_5,$$

$$y_5' = \left(-\frac{3}{4}y_1y_5 - Nby_7y_5 - Nty_5^2\right) y_6' = y_7,$$

$$y_7' = \frac{-3}{4}Ley_1y_7 - \frac{Nt}{Nb}y_5', \tag{54}$$

with the boundary conditions

$$y_1(0) = y_2(0) = 0 \text{ and } y_4(0) = y_6(0) = 1. \tag{55}$$

To solve (54) with (55) as an initial value problem, we need the values for $y_3(0)$ i.e. $s''(0)$, $y_5(0)$ i.e. θ′(0), and $y_7(0)$ i.e. $f'(0)$, but no such values are given. The initial guess values for $s''(0), \theta'(0)$, and $f'(0)$ are chosen, and the fourth-order Runge–Kutta integration scheme is applied to obtain the solution. Then, we compare the calculated values of $s'(\eta), \theta(\eta)$,and $f(\eta)$at η_∞ with the given boundary conditions $s'(\eta_\infty) = 0$, $\theta(\eta_\infty) = 0$, and $f(\eta_\infty) = 0$and adjust the values of $s''(0)$, $\theta'(0)$, and $f'(0)$ using the shooting technique to give a better approximation for the solution. The process is repeated until we get the correct results up to the desired accuracy level of10^{-8}, which fulfils the convergence criterion.

6. Results and discussion

The analytical solutions for the hydromagnetic flow of an incompressible viscous nanofluid over a vertical plate were obtained using the HAM method. The obtained analytical solutions were verified by the numerical solutions obtained using the fourth-order Runge–Kutta method. The results are displayed with the help of graphical illustrations. To test the accuracy of these analytical and numerical solutions, we compared the resulting calculated values with those reported in Bejan [34]. The comparison, shown in Table 1,was found to be in good agreement.

The effects of the Prandtl number and magnetic parameter on the dimensionless velocity profile along the vertical plate are shown in Fig. 2. A comparison of the velocity profiles for the two different Prandtl numbers shows that the velocity profile rises as *Pr* increases, unlike for the flow of a regular fluid over a vertical plate [16]. It also shows that the presence of the magnetic parameter reduces the dimensionless velocity. This is due to the fact that, when a transverse magnetic field is applied to an electrically conducting fluid, it gives rise to a resistive force known as the Lorentz force. This force causes the fluid to experience resistance by increasing the friction between its layers, which

decreases velocity. Thus, the increasing values of the magnetic parameter decrease the velocity of the nanofluid.

Fig. 3 shows the effects of the buoyancy ratio on the dimensionless velocity profile in the presence of a magnetic field. The velocity profile decreases as the buoyancy ratio increases. Fig. 4 shows the effects of the Lewis number on the dimensionless velocity profile in the presence of a magnetic field for the selected parameters. It is clear that the velocity is enhanced as the Lewis number increases. Fig. 5 shows the effects of Brownian motion and thermophoresis parameters on the dimensionless velocity profile. It can be seen that the increasing values of *Nb* and *Nt* enhance the velocity profile of the nanofluid.

The effects of the magnetic parameter on the dimensionless temperature profile along the vertical plate are shown in Fig. 6. It can be seen that the increasing values of the magnetic parameter causes the nanofluid to become warmer and, therefore, increase in temperature, which is similar to the temperature profile in the natural convective boundary layer of a regular fluid. Fig. 7 displays the effects of the Prandtl number on the temperature profile. It can be noted that the temperature decreases with the increasing values of the Prandtl number. This is due to the fact that the thermal boundary-layer thickness decreases with an increase in the Prandtl number.

Fig. 8 demonstrates the effects of the buoyancy ratio on the dimensionless temperature profile in the presence of magnetic field. From this figure, it is apparent that the temperature increases as the buoyancy ratio increases. Fig. 9 depicts the effects of the Lewis number on the dimensionless temperature profile in the presence of a magnetic field. It can be observed that the increasing values of *Le* decrease the temperature profile. Fig. 10 illustrates the dimensionless temperature profile in the presence of magnetic field and nanofluid parameters for different values of the Brownian motion and thermophoresis parameters. It can be noted that the Brownian motion and thermophoresis parameters augment the temperature profile. This is because increasing *Nt* means a higher thermophoresis force, which tends to move nanoparticles from hot to cold areas and consequently increases the fluid temperature.

The magnetic parameter's effect on the dimensionless concentration profile along the vertical plate is shown in Fig. 11. From the figure, it can be seen that the dimensionless nanosolid fraction increases as the magnetic parameter increases. Fig. 12 shows the effects of the Prandtl number on the dimensionless nanoparticle volume fraction. It can be observed that the nanoparticle volume fraction decreases as the Prandtl number increases.

Fig. 13 depicts the effects of the buoyancy ratio on the dimensionless nanoparticle volume fraction profile. The nanoparticle volume fraction increases as the buoyancy ratio increases.

Fig.14 shows the effect of the Lewis number on the dimensionless nanoparticle volume fraction profile in the presence of a magnetic field. It is interesting to note that the increasing values of *Le* decrease the nanoparticle volume fraction. Close observation of Figs. 9 and 14 revealed that the increasing values of the Lewis number arrest the concentration boundary-layer thickness.

Fig. 15 exhibits the effects of the Brownian motion and thermophoresis parameters on the dimensionless nanoparticle volume fraction profile in the presence of a magnetic field. It is clear that an increase in the values of both nanofluid parameters, thermophoresis and Brownian motion, causes a decrease of the nanosolid fraction. Due to the presence of nanoparticles in a nanofluid system, Brownian motion of the particles takes place, and by increasing it, the heat-transfer characteristics of the fluid changes, which results in increased temperature. Moreover, a slight decrease in the nanoparticle volume boundary-layer thickness is observed with increasing *Nb*.

Figs. 16 and 17 show the effects of the Brownian motion parameter, thermophoresis parameter, magnetic parameter, and Lewis number on the reduced Nusselt number and local Sherwood number, respectively. It can be noted that the reduced Nusselt number decreases with magnetic parameter, Brownian motion parameter, thermophoresis parameter, and Lewis number (Fig. 16).

The local Sherwood number decreases with magnetic parameter and increases with Brownian motion parameter, thermophoresis parameter, and Lewis number (Fig. 17).

Table 2 shows the values of the reduced Nusselt and Sherwood numbers. The reduced Nusselt and Sherwood numbers decrease with the increasing values of *Nr* and *M*. The increasing values of *Pr* increase both the reduced Nusselt and Sherwood numbers. The parameters *Nb* and *Le* decrease the values of the Nusselt number and increase the Sherwood number. Table 2 provides the information

about the heat- and mass-transfer characteristics of the flow in a convenient form for research and engineering calculations.

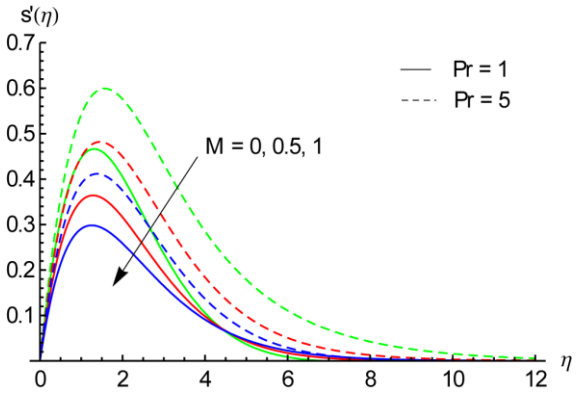

Fig.2 Effects of the magnetic parameter and Prandtl number on the dimensionless velocity for Le = 1 and Nb = Nt = Nr = 0.1.

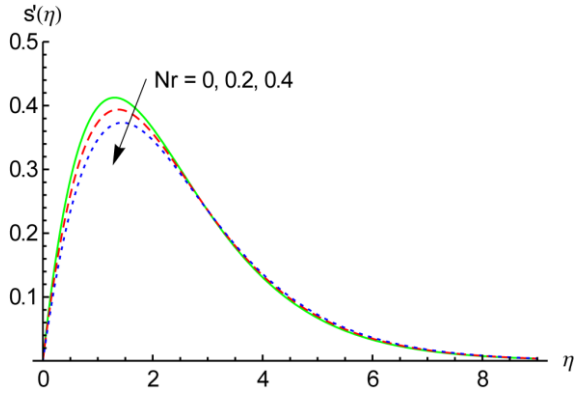

Fig.3 Effects of the buoyancyratio on the dimensionless velocity profiles for Pr = 1, Le = 10, M = 0.5, and Nb = Nt = 0.1.

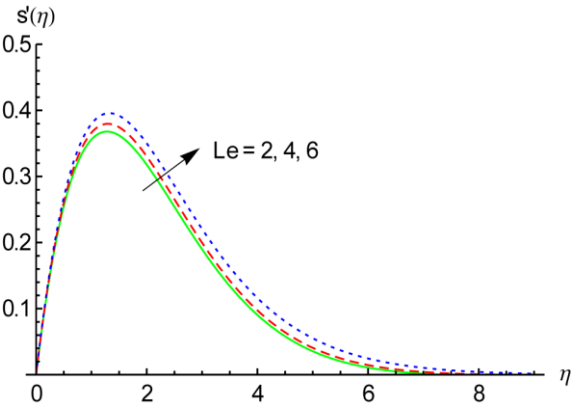

Fig.4 Effects of the Lewis number on the dimensionless velocity profiles for Pr = 1, M = 0.5, and Nb = Nt = Nr = 0.1.

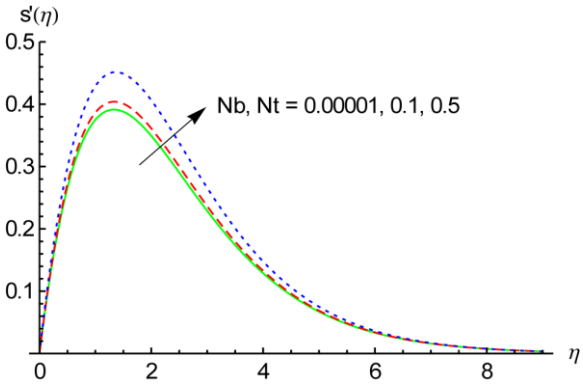

Fig.5 Effects of Brownian motion and thermophoresis parameters on dimensionless velocity profiles for Pr = 1, Le = 10, M = 0.5, and Nr = 0.1.

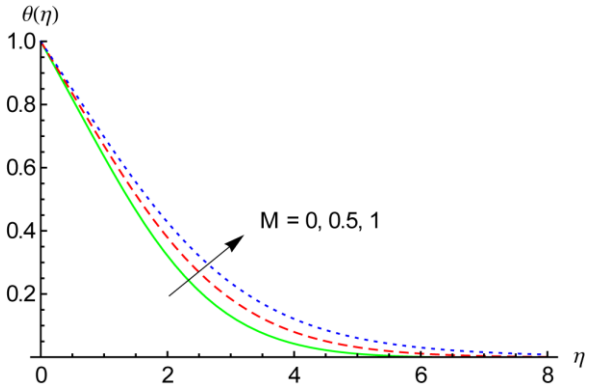

Fig.6 Effects of the magnetic parameter on the dimensionless temperature profiles for Pr = 1, Le = 1, and Nb = Nt = Nr = 0.1.

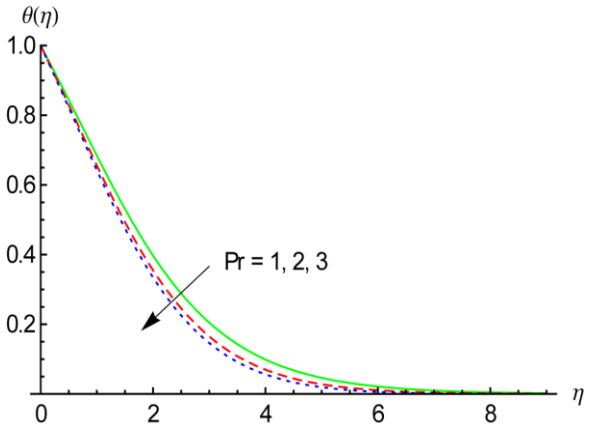

Fig.7 Effects of the Prandtl number on the temperature profiles for M = 0.5, Le = 1, and Nb = Nt = Nr = 0.1.

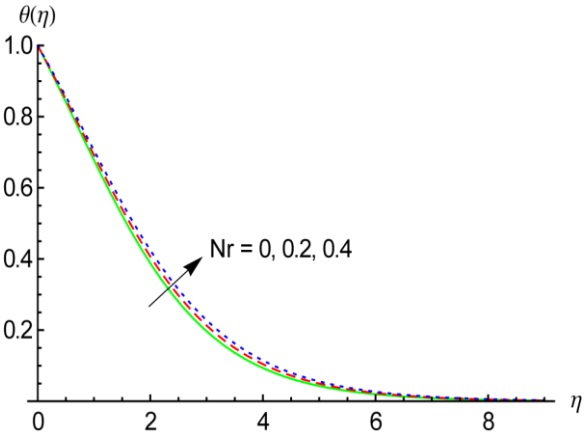

Fig.8 Effects of the buoyancy ratio on the dimensionless temperature profiles for Pr = 1, Le = 10, Nb = Nt = 0.1, and M = 0.5.

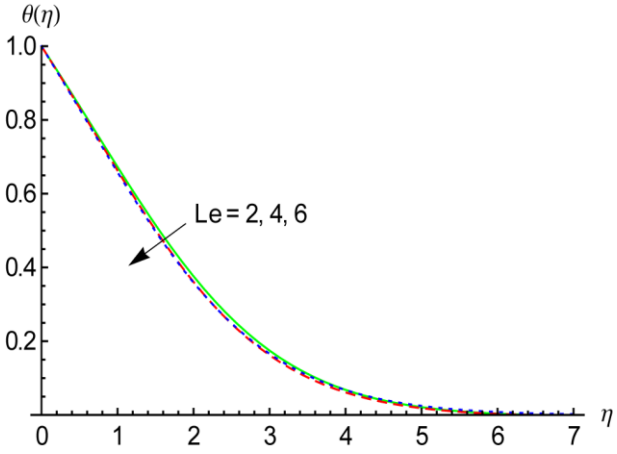

Fig.9 Effects of the Lewis number on the dimensionless temperature profiles for Pr = 1, Nb = Nt = Nr = 0.1, and M = 0.5.

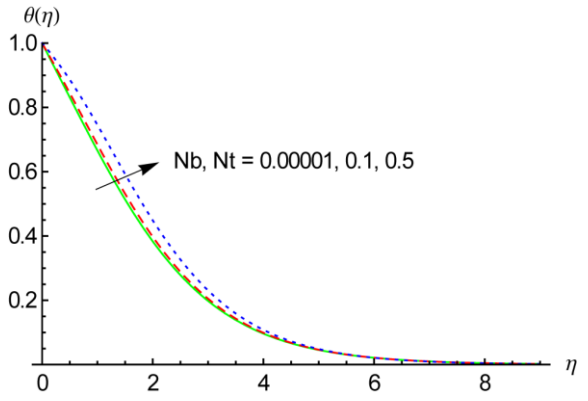

Fig.10 Effects of Brownian motion and thermophoresis parameters on the dimensionless temperature profiles for Pr = 1, Le = 10, M = 0.5, and Nr = 0.1.

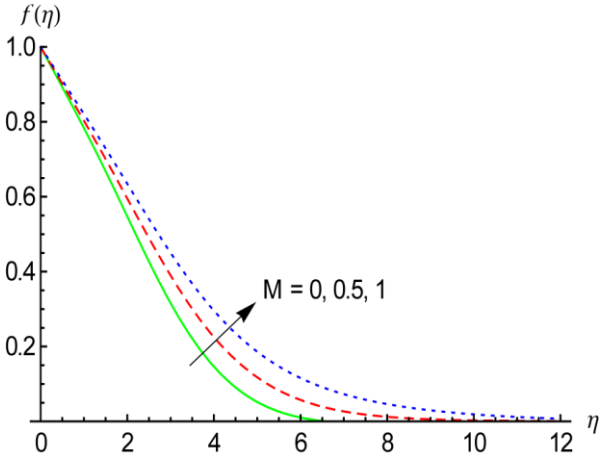

Fig.11 Effects of themagnetic parameter on the dimensionless solid volume fraction of the nanofluid profiles for Pr = 1, Le = 1, and Nb = Nt = Nr = 0.1.

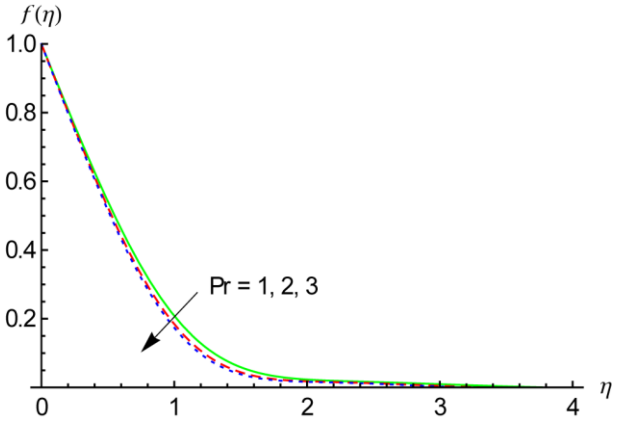

Fig.12 Effects of the Prandtl number on the dimensionless solid volume fraction of the nanofluid profiles for Pr = 1, Le = 1, and Nb=Nt=Nr=0.1.

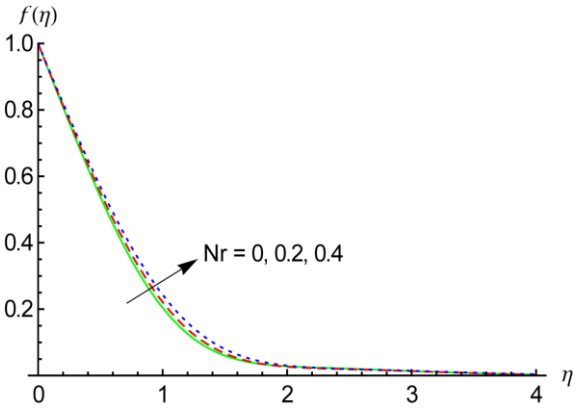

Fig.13 Effects of buoyancyratio on the dimensionless solid volume fraction of the nanofluid profiles for Pr = 1, Le = 10, Nb = Nt = 0.1, and M = 0.5.

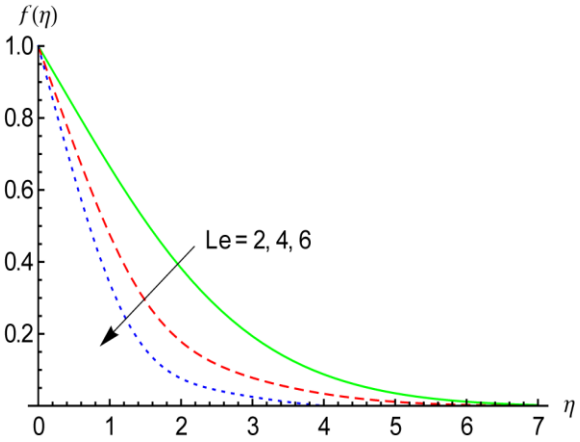

Fig.14 Effects of the Lewis number on the dimensionless solid volume fraction of the nanofluid profiles for Pr=1, Nb = Nt = Nr = 0.1, and M = 0.5.

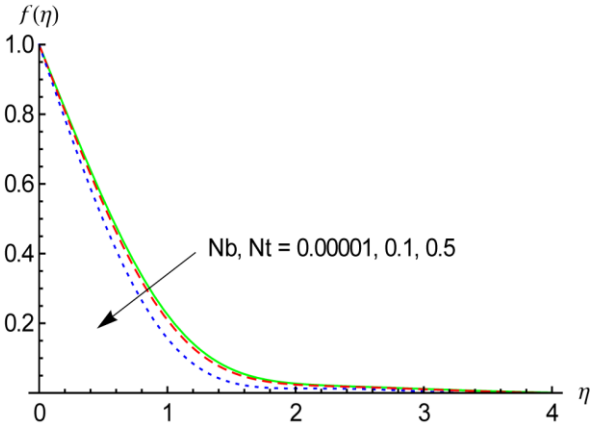

Fig.15 Effects of the Brownian motion parameters on the dimensionless temperature profiles for Pr = 1, Le = 10, M = 0.5, and Nt = Nr = 0.1.

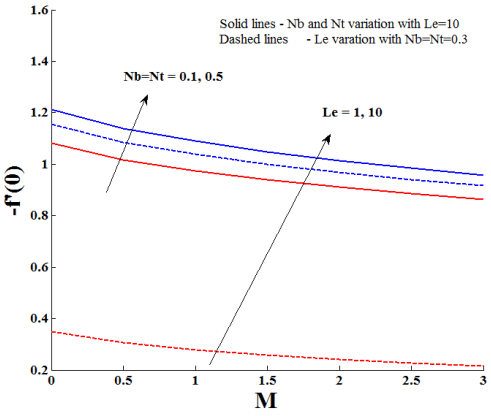

Fig.16 Effects of Brownian motion parameters, the Lewis number and magnetic parameter on the reduced Nusselt number for Pr = 7 and Nr = 0.1.

Table 1. Comparison test results. Values of the reduced Nusselt number $Nur = Ra_x^{1/4}\ Nu$ in the limiting case of a regular fluid. The present results are with Le = 10 and $Nr = Nb = Nt = 10^{-5}$.

Pr	**Bejan [34]**	**Present results (absence of magnetic parameter)**	
		Analytical	Numerical
1	0.401	0.40103	0.40102817
10	0.465	0.46496	0.46496287
100	0.490	0.49000	0.49000028

Table 2. Variation of Nur and Shr with Pr, Nb, and Nr for Nt = 0.1 and Le = 10.

Le	**M**	**Nb**	**Nr**	**Pr=1**				**Pr=5**			
				Nur		Shr		Nur		Shr	
				Analytical	Numerical	Analytical	Numerical	Analytical	Numerical	Analytical	Numerical
10	0	0.1	0.1	0.35423	0.35422747	1.00337	1.00336781	0.39913	0.39912839	1.07059	1.07058521
			0.3	0.34768	0.34767813	0.97818	0.97818444	0.39186	0.39186369	1.04546	1.045461295

			0.5	0.34059	0.34058452	0.95061	0.95060987	0.38405	0.38404555	1.01815	1.01814560
10	0	0.1	0.1	0.35423	0.35422747	1.00337	1.00336781	0.39913	0.39912839	1.07059	1.07058521
		0.3		0.30478	0.30478323	1.05170	1.05170420	0.34438	0.34437949	1.12009	1.12008705
		0.5		0.26100	0.26100299	1.06575	1.06575282	0.29570	0.29569842	1.13521	1.13520899
10	0	0.1	0.1	0.35423	0.35422747	1.00337	1.00336781	0.39913	0.39912839	1.07059	1.07058521
	1			0.287352	0.28735186	0.86314	0.86313586	0.33916	0.33915732	0.95827	0.95827136
	2			0.24690	0.24690692	0.77458	0.77458149	0.30419	0.30418486	0.89014	0.89013613
10	1	0.1	0.1	0.287352	0.28735186	0.86314	0.86313586	0.33916	0.33915732	0.95827	0.95827136
12				0.28715	0.28714701	0.93599	0.93598525	0.33888	0.33888312	1.03576	1.03576257
14				0.28697	0.28697711	1.00044	1.00044277	0.33865	0.33865419	1.10433	1.10433227

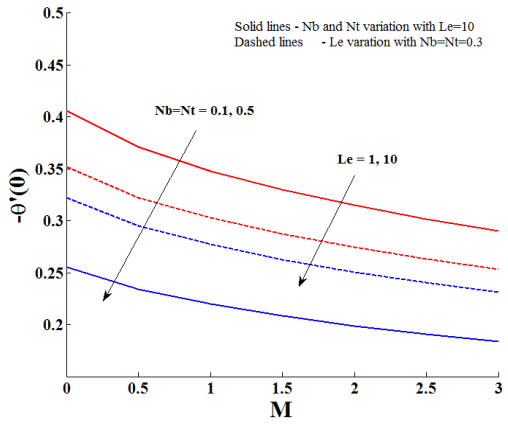

Fig.17 Effects of the Brownian motion parameters, Lewis number, and the magnetic parameter on the local Sherwood number for Pr = 7 and Nr = 0.1.

7. Conclusion

The hydromagnetic flow of an electrically conducting nanofluid past a vertical plate was studied both analytically and numerically. The governing equations for this investigation were solved analytically using the HAM, and the results were verified using numerical solutions obtained by the fourth-order Runge–Kutta method along with the shooting technique. The following specific conclusions were derived from this study:

- It was found that the dimensionless velocity increases with the decrease of the magnetic parameter. The temperature and the concentration profiles increase with the increasing values of the magnetic parameter. The increasing values of the Prandtl number increase the velocity profile and decrease the temperature and solid volume fraction profiles in the flow region.
- It was noted that the Brownian motion and thermophoresis parameters enhance the velocity of the temperature profiles but suppress the concentration profile.
- The increasing values of the buoyancy ratio decrease the velocity profile and increase the temperature and concentration profiles in the flow region.
- The Nusselt number decreases with the magnetic parameter, Brownian motion parameter, thermophoresis parameter, and Lewis number
- The local Sherwood number decreases with the magnetic parameter and increases with the Brownian motion parameter, thermophoresis parameter, and Lewis number.

Nomenclature

D_B Brownian diffusion coefficient

D_T Thermophoretic diffusion coefficient

f rescaled nanoparticle volume fraction

g gravitational acceleration vector

k thermal conductivity

Le Lewis number

M magnetic parameter

Nr buoyancy-ratio parameter

Nb Brownian motion parameter

Nt thermophoresis parameter

Nur reduced Nusselt number

Pr Prandtl number

Ra_x local Rayleigh number

T temperature

T_w temperature at the vertical plate

T_∞ ambient temperature

(x,y) Cartesian coordinates

Greek symbols

α Thermal diffusivity

β volumetric expansion coefficient η similarity variable

θ	dimensionless temperature
μ	dynamic viscosity of the fluid
ν	kinematic viscosity
ρ_f	fluid density
ρ_p	nanoparticle mass density
$(\rho c)_f$	heat capacity of the fluid
$(\rho c)_p$	effective heat capacity of the nanoparticle material
ϕ	nanoparticle volume fraction
ϕ_w	nanoparticle volume fraction at the vertical plate
ϕ_∞	ambient nanoparticle volume fraction, attained as y, tends to infinity
ψ	stream function

Acknowledgments

The authors wish to express their sincere thanks to the honorable referees for their valuable comments and suggestions to improve the quality of the paper.

References

[1] S.U.S. Choi, Enhancing thermal conductivity of fluids with nanoparticles, {in: D A. Siginer, H.P. Wang (Eds.), Developments and Applications of Non-Newtonian Flows, ASME FED, 231/MD (66)}, 66, 99-105, (1995).

[2] J. Boungiorno, et al., A benchmark study of thermalconductivity of nanofluids,J. Appl. Phys., 106paper 094312,(2009).

[3] J. Buongiorno, Convective transport in nanofluids, J. Heat Transfer, 128 (2006) 240-250.

[4] P. Rana,R. Bhargava , Flow and heat transfer of a nanofluid over a nonlinearly stretching sheet: a numerical study. Commun. Nonlinear Sci. Numer. Simulat., 17, 212-226,(2012).

[5] M.A.A Hamad, Analytical solution of natural convection flow of a nanofluid over a linearly stretching sheet in the presence of magnetic field, Int. Comm. Heat Mass Transfer., 38, 487-492, (2011).

[6] A.J. Chamkha and A.M. Aly, MHD Free Convection Flow of a Nanofluid past a Vertical Plate in the Presence of Heat Generation or Absorption Effects. Chem. Eng, Commun., 198, 425-441, (2011).

[7] A.J. Chamkha, A.M. Rashad, and E. Al-Meshaiei, "Melting Effect on Unsteady Hydromagnetic Flow of a Nanofluid Past a Stretching Sheet." Int. J. of Chem. Reactor Eng., 9:A113, (2011).

[8] A.J. Chamkha, A.M. Aly, H. Al-Mudhaf, Laminar MHD Mixed Convection Flow of a Nanofluid along a Stretching Permeable Surface in the Presence of Heat Generation or Absorption Effects, International Journal of Microscale and Nanoscale Thermal and Fluid Transport Phenomena, 2, 51-70, (2011).

[9] R.S.R. Gorla and A.J. Chamkha, Natural Convective Boundary Layer Flow over a Horizontal Plate Embedded in a Porous Medium Saturated with a Non-Newtonian Nanofluid." International Journal of Microscale and Nanoscale Thermal and Fluid Transport Phenomena, 2, 211- 227, (2011).

[10] R.S.R. Gorla, A.J. Chamkha and A. Rashad, Mixed Convective Boundary Layer Flow over a Vertical Wedge Embedded in a Porous Medium Saturated with a Nanofluid: Natural Convection Dominated Regime. Nanoscale Research Letters, 6 (207), 1-9, (2011).

[11] N. Vishnu Ganesh, B. Ganga, A.K. Abdul Hakeem, Lie symmetry group analysis of magnetic field effects on free convective flow of a nanofluid over a semi infinite stretching sheet, J. Egyptian Math. Soc., 22, 304-310,(2014).

[12] N. Vishnu Ganesh, A. K. Abdul Hakeem , R. Jayaprakash , and B. Ganga, \break Analytical and Numerical Studies on Hydromagnetic Flow of Water Based Metal Nanofuids Over a Stretching Sheet with Thermal Radiation Effect, J. Nanofluids , 3, 154-161, (2014).

[13] M. Govindaraju, N. Vishnu Ganesh, B. Ganga, A.K. Abdul Hakeem, Entropy generation analysis of magneto hydrodynamic flow of a nanofluid over a stretching sheet., J. Egyptian Math. Soc.,429-434(2014).

[14] M.M. Rashidi, N.Vishnu Ganesh , A.K. Abdul Hakeem and B. Ganga, Buoyancy Effect on MHD Flow of Nanofluid over a Stretching Sheet in the Presence of Thermal Radiation, J. Mol. liq., 234-238, (2014).

[15] A.K. Abdul Hakeem, N.Vishnu Ganesh, B.Ganga, Magnetic field effect on second order slip flow of nanofluid over a stretching/shrinking sheet with thermal radiation effect, J. Magn. Magn. Mater., 381, 243-257 (2015).

[16] A.V. Kuznetsov, D.A. Nield, Natural convective boundary layer flow of a nanofluid past a vertical plate. Int. J. Therm. Sci., 49, 243-247, (2010).

[17] A.V. Kuznetsov, D.A. Nield, Double-diffusive natural convective boundary-layer flow of a nanofluid past a vertical plate. Int. J. Therm. Sci., 50, 712-717, (2011).

[18] W.A. Khan, I. Pop, Boundary-layer flow of a nanofluid past a stretching sheet, Int. J. Heat Mass Transfer, 53,2477-2483, (2010).

[19] W.A. Khan, A. Aziz, Natural convection flow of a nanofluid over a vertical plate with uniform surface heat flux, Int. J. Therm. Sci., 50(7), 1207-1214, (2011).

[20] R.S.R. Gorla, A. Chamkha, Natural convective boundary layer flow over a horizontal plate embedded in a porous medium saturated with a nanofluid. J. Modern Phy., 2,62-71, (2011).

[21] A. Aziz, W.A. Khan, Natural convective boundary layer flow of a nanofluid past a convectively heated vertical plate, Int. J. Therm. Sci., 52, 83-90, (2012).

[22] F. S. Ibrahim, M. A. Mansour, M. A. A. Hamad, Lie group analysis of radiative and magnetic field effects on free convection and mass transfer flow past a semi-infinte vertical flat plate, Electronic Journal of Differential Equations, 39, 1-17, (2005).

[23] R.Muthucumaraswamy, B.Janakiraman, MHD and radiation effects on moving isothermal vertical plate with variable mass diffusion, Theoret. Appl. Mech., 33, 17-29, (2006).

[24] H. Yahyazadeh, D. D. Ganji, A. Yahyazadeh, M. T. Khalili, P. Jalili, and M. Jouya, Evaluation of natural convection flow of a nanofluid over a linearly stetching sheet in the presence of magnetic field by the Differential Transformation Method, Thermal Science, 16, 1281-1287, (2012).

[25] S.J. Liao, Beyond perturbation: Introduction to the homotopy analysis method, BocaRaton: Chapman Hall CRC Press,(2000).

[26] S.J. Liao, On the homotopy analysis method for nonlinear problems, Appl. Math. Comput., 147, 499-513, (2004).

[27] S.J. Liao, Y. Tan, A general approach to obtain series solutions of nonlinear differential equations, Stud. Appl. Math. , 119,297-355, (2007).

[28] S. Dinarvand, M.M. Rashidi, A Reliable Treatment of Homotopy Analysis Method for Two-Dimensional Viscous Flow in a Rectangular Domain Bounded by Two Moving Porous Walls, Nonlinear Analysis: Real World Applications 11 (3), 1502-1512, (2010).

[29] M.M. Rashidi, S.A. Mohimanian Pour, Analytic Approximate Solutions for Unsteady Boundary-Layer Flow and Heat Transfer due to a Stretching Sheet by Homotopy Analysis Method, Nonlinear Analysis: Modelling and Control 15 (1), 83-95, (2010).

[30] O. Anwar Bég, M.M. Rashidi, T.A. Bég, M. Asadi, Homotopy Analysis of Transient Magneto-Bio-Fluid Dynamics of Micropolar Squeeze Film in a Porous Medium: a Model for Magneto-Bio-Rheological Lubrication, J. Mechanics in Medicine and Biology, 12 (03), (2012).

[31] M.M. Rashidi, O. Anwar Bég, M.T. Rastegari, A Study of Non-Newtonian Flow and Heat Transfer over a Non-Isothermal Wedge Using the Homotopy Analysis Method, Chem. Eng. Communications 199 (2), 231-256, (2012).

[32] M.M. Rashidi, S.A. Mohimanian Pour, T. Hayat, S. Obaidat, Analytic Approximate Solutions for Steady Flow over a Rotating Disk in Porous Medium with Heat Transfer by Homotopy Analysis Method, Comput.Fluids 54, 1-9, (2012).

[33] M.M. Rashidi,·N. Freidoonimehr,·A. Hosseini, O. Anwar Bég,·T.-K. Hung, Homotopy Simulation of Nanofluid Dynamics from a Non-Linearly Stretching Isothermal Permeable Sheet with Transpiration, Meccanica, 49 (2),469-482, (2014).

[34] A Bejan, Convection Heat Transfer, Wiley, New York, NY, (1984).